# Chitin nanocrystals as Pickering stabilizer for O/W emulsions: Effect of the oil chemical structure on the emulsion properties

Fatma Ben Cheikh, Ayman Ben Mabrouk, Albert Magnin, Jean-Luc Putaux, Sami Boufi

# Chitin nanocrystals as Pickering stabilizer for O/W emulsions: Effect of the oil chemical structure on the emulsion properties

Fatma Ben Cheikh[a], Ayman Ben Mabrouk[a], Albert Magnin[b], Jean-Luc Putaux[c], Sami Boufi[a,*]

[a] University of Sfax, LMSE, Faculty of Science, BP 802, 3018 Sfax, Tunisia

[b] Univ. Grenoble Alpes, CNRS, Grenoble INP, LRP, F-38000 Grenoble, France

[c] Univ. Grenoble Alpes, CNRS, CERMAV, F-38000 Grenoble, France

*Corresponding author: sami.boufi@fss.rnu.tn*

Published in: **Colloids and Surfaces B: Biointerfaces** *200* (2021), 111604

DOI: 10.1016/j.colsurfb.2021.111604

## Abstract

Chitin nanocrystals (ChNCs) produced by hydrochloric acid hydrolysis of chitin were used as stabilizing agent for oil-in-water (O/W) emulsification of soybean oil (SO), acrylated soybean oil (ASO), and epoxidized soybean oil (ESO). The emulsion stability, droplet size, and rheology of the emulsion were found to be significantly affected by the oil chemical structure. Strong interaction between ChNCs and the oil droplets enhanced the stabilizing efficiency of ChNCs through a Pickering effect, resulting in emulsions with low droplet size and long-term stability. The use of ChNCs as stabilizer for O/W emulsions in replacement of synthetic surfactants opens new avenues to produce emulsions for a wide variety of applications, including cosmetic products, coating, inks and adhesives.

***Keywords**:* Pickering emulsions, chitin nanocrystals, oil-in-water emulsion, soybean oil

## 1. Introduction

Emulsions, which refer to dispersions of an immiscible liquid phase within a second host liquid phase, find widespread uses in broad areas of applications, such as paints and inks, cosmetics, pharmaceuticals as a vehicle for therapeutic drugs, agricultural as a vehicle for insecticides, pesticides and fungicides, and food for oil and fat emulsification.

Emulsions are thermodynamically unstable and the addition of a stabilizer is a prerequisite to prevent a phase separation induced by the fusion of oil droplets during storage. The role of the stabilizer is to provide enough energy barrier at the oil-water interface by forming a protective layer capable of hindering the coalescence and aggregation of droplets [1]. Typically, this property is mostly provided by synthetic surfactants which are known to act through different effects:(i) lowering of the interfacial tension to facilitate the emulsification process, (ii) generation of a steric or electrostatic barrier to offset the attractive forces, and (iii) enhancement of the dilatational elasticity of the O/W interface [2]. An alternative for emulsification is the use of solid particles capable of adsorbing at the oil–water interface, thus providing stabilization through the so-called Pickering effect [3]. The obvious benefits of this class of emulsions are to mitigate the shortcoming of synthetic surfactants, such as irritancy in cosmetic products, water sensitivity and optical effect for coating, hazardousness for aquatic ecosystems, and biocompatibility for healthcare. In this sense, the use of biobased nanoparticles (NPs) derived from renewable biodegradable materials as Pickering stabilizers would be of paramount interest. A wide variety of biobased NPs with different morphologies and from different origins has been explored. Nanocellulose with different morphologies and chemical functionalities, including cellulose nanocrystals (CNCs) [4], bacterial cellulose (BC)[5], cellulose nanofibrils (CNFs) [6], and hydrophobized CNFs, were among the first biobased NPs to be explored as stabilizers for O/W or W/O emulsions depending on their hydrophilic-hydrophobic balance [7]. Starch nanocrystals (SNCs) and starch nanoparticles (SNPs) have also shown potential as stabilizers in Pickering emulsions and in heterogeneous polymerization (emulsion and miniemulsion) [8]. Recent work has shown that the esterification of SNCs with octenyl succinic acid at a low substitution degree (as low as 0.012) enhanced the emulsifying aptitude for stabilization of O/W emulsions [9]. Four publications have also been reported on surfactant-free Pickering emulsion and miniemulsion polymerization of acrylic monomers in the presence of SNCs and SNPs as sole stabilizers [10,11,12,13].

The main mechanism accounting for the Pickering stabilization is the irreversible adsorption of solid particles at the oil-water interface, providing a steric barrier against droplet coalescence

and Ostwald ripening [14]. This is mostly the case when the solid particles have a good wettability for the oil phase, resulting in the generation of a dense layer of adsorbed particles around droplets. Under this condition, the energy barrier against the coalescence of oil droplets corresponds to the energy involved to expel the particles from the interface. Other contributions to the stabilization process include electrostatic repulsion induced by charged particles, or the setup of a three-dimensional network in the continuous phase generated by the solid particles that entrap the dispersed droplets and limit their movement [15].

Nanochitins, that includes chitin nanofibers (ChNFs) and chitin nanocrystals (ChNCs), constitute another class of biobased nanoparticles attracting much interest in Pickering emulsion applications. Chitin, a $\beta$-(1→4)-linked 2-amino-2-deoxy-D-glucosamine, is a naturally abundant polysaccharide typically isolated from crustacean shells and from fungi sources [16]. Nanochitins combine the unique properties of native chitin including nontoxicity, biocompatibility, biodegradability, chemical stability and antibacterial activity [17] with the attributes of nanosize materials (i.e. low density, large surface and surface reactivity).

The first work on the possibility of using ChNCs in emulsions was reported by Tzoumaki et al. [18]who produced corn O/W emulsions stabilized by ChNCs and investigated the effect of ChNC concentration, ionic environment, pH and temperature on the emulsion properties. Since then, several articles have described the emulsification potential of nanochitins to produce nanocomposites [19,20], food emulsions [21], functional materials [22], foams [23], among others. Recently, stable O/W high-internal-phase (HIPE) Pickering emulsions stabilized solely by ChNCs were produced at a volume fraction amounting 88% [24,25]. The stabilization mechanism was explained by the adsorption of ChNFs in close-packed layers on the droplets at the oil-water interface, and the generation of a ChNF network in the continuous phase. By an appropriate choice of aspect ratio of ChNFs and their deacetylation degree, highly stable concentrated emulsions with fine droplets were produced using a ChNF content as low as 0.01wt%[26]. Although many papers have demonstrated the ability of ChNCs to stabilize O/W emulsions via a Pickering effect, in most them however, only one type of oil was used, generally being highly apolar. The evolution of the emulsion properties according to the oil type has not been yet investigated.

In the present work, the efficiency of ChNCs to stabilize emulsions based on soybean oil (SO), acrylated soybean oil (ASO), and epoxidized soybean oil (ESO) was investigated, and the properties of the resulting emulsions were characterized in terms of particle size, rheology and stability over time. The main emphasis was to understand how the structure of the oil likely affected its aptitude to obtain O/W emulsions.

## 2. Experimental section

*2.1. Materials*

Chitin from crab shells and hydrochloric acid (HCl, 37vol%, reagent grade) were purchased from Sigma-Aldrich Chemicals. Soybean oil (SO) was a commercial edible product with the following composition (15.7 % saturated fatty acids, 25.8% oleic acid, 51.3 linoleic acid and 7.2% linolenic acid, determined by gas chromatography). Epoxidized soybean oil (ESO) (Vikoflex 7170 from Arkema, with an epoxy content of 6.2% and acid value 0.5 max) and acrylated soybean oil (ASO) (CN111 from Arkema) Deionized water was used. The chemical structure of the different oils is given in **Figure 1S**.

*2.2. Chitin nanocrystal preparation*

Chitin nanocrystals (ChNCs) were prepared by sulfuric acid hydrolysis of crude chitin from crab shells as described in details in previous works [27]. Briefly, 4 g of chitin was added to 4 M aqueous HCl solution and left under magnetic stirring during 90 min at 95 °C. After cooling to 20 °C, 150 mL of water was added and the suspension was centrifuged at 5,000 rpm to recover the ChNCs. The ChNC suspension was then dialyzed with water to reach a constant pH value. A stock suspension of ChNCs at 4 wt% solid content and pH 4-5 was used for the emulsification process.

*2.3. Degree of deacetylation (DD)*

The DD was determined by conductometric titration following the method described by Raymond et al.[28]. An aqueous ChNC suspension (about 100 mg dry weight) was brought to pH 3 by addition of a 0.01N HCl solution and titrated with a 0.005 M NaOH solution by monitoring the conductance as a function of added NaOH. The DD was calculated from **Eq. 1**:

$$DD = 203 \times (V_2 - V_1)\frac{N}{m+42(V_2 - V_1)N}100 \qquad (1)$$

where $N$ is the NaOH concentration, $V_2$ and $V_1$ are the equivalent volume of NaOH at the two inflection points; $m$ is the mass of dry ChNCs. The titration plot is given in **Figure 2S**.

*2.4. Emulsion preparation*

Three grams of oil was added to 17 mL of the aqueous ChNC suspension at pH 5 and mixed by vortexing during 1 min, followed by sonication during 1 min at a 60% amplitude (Sonics Vibracel Model CV33) in a cold water bath. The final pH of the emulsion was around 5.

*2.5. Droplet size measurement*

The droplet size in the emulsion was measured at 25 °C using a Malvern ZS Zetasizer instrument at a fixed scattering angle of 173°. Measurements were made on emulsions diluted to about 5% by addition of water. Briefly, 1 mL of the emulsion was diluted by addition of 2 mL of water. After manual gentle mixing to homogenize the emulsion, the sample was immediately analyzed. The size was expressed as a Z-average which corresponds to the diameter of an equivalent hard sphere with similar diffusion coefficient as that of the measured particle. All measurements were performed in triplicate and the values were averaged to obtain the mean diameter.

*2.6. Zeta potential measurement*

ζ-potential measurements were performed at 25 °C using a laser Doppler electrophoresis apparatus (Malvern Zetasizer ZS, UK). All measurements were determined at the same ionic strength of 0.001 M, using a KCl solution.

*2.7. Transmission electron microscopy (TEM)*

Drops of ChNC suspensions (0.001 wt%)were deposited onto carbon-coated copper grids freshly glow-discharged in a Pelco easiGlow station. A drop of 2 wt% uranyl acetate negative stained was deposited before complete drying. The stain in excess was removed and the preparation allowed to air-dry. The specimens were observed with a JEOL JEM 2100-Plus microscope operated at 200 kV and images were recorded using a Gatan Rio 16 camera.

*2.8. Scanning electron microscopy (SEM)*

The Irgacure 184 photoiniator (1 %) was incorporated in the ASO oil and the Pickering emulsion prepared in the presence of ChNCs was irradiated with UV light to induce crosslinking in the oil, rigidify the droplets, and prevent the flowing of the oil in the dry preparations. The emulsion was gently centrifuged and the clear supernatant was taken out to remove the excess free ChNCs. The particles were resuspended in water and the treatment was repeated twice. A drop of the emulsion was deposited on carbon tape. After drying, the specimen was coated with Au/Pd in a Baltech MED-020 sputter coater and observed in secondary electron mode in a Thermo Scientific Quanta 250 microscope equipped with a field emission gun and operating at 2.5 kV.

*2.9. Rheological measurements*

The rheological measurements were performed on a Kinexus Pro+rheometer (Malvern Instruments, UK) using a plate-plate geometry with a diameter of 25 mm with a rough surface to

prevent slippage to the wall. The temperature was kept constant at 25 °C using Peltier heating system. Under dynamic mode, the linear domain was first determined by a sweep of the storage modulus G' and loss modulus G" *vs.* strain. The strain range extended from 0.01 to 100%.Then,a frequency sweep at a fixed strain in the elastic linear domain was made. In shear rate measurement, a cone plate geometry was used (cone angle, 2°; diameter, 20 mm; truncation, 56 μm) with a ramp from 0.01 to 100 $s^{-1}$.To prevent any risk of slippage, the surfaces of rheometric tools have been roughened [29].

*2.10. Contact angle measurement*

ChNC films were prepared by casting 0.5 wt% ChNC suspensions, previously sonicated in a bath for 10 min, in a Petri-dish and drying at 40 °C for two days until complete evaporation of water. A transparent film, about 100 μm-thick, was obtained. Contact angle measurements were carried out by deposing a calibrated water droplet on the thin films using OCA 15 Drop Shape Analyzer from Dataphysics, equipped with a high-resolution CCD camera, working at an acquisition of 50 images per second and data were analyzed with the OCA software.

*2.11. Surface tension measurement*

The surface tension of ChNC suspensions at different concentrations was measured using a Kruss tensiometerK100 (Hamburg, Germany) with a Du Nouy ring at 25 °C. The measurements were performed in 5 replicates and the result was averaged.

## 3. Results and discussion

*3.1. Morphology and colloidal properties of ChNCs*

ChNCs were produced by acid hydrolysis with a yield close to 20 wt% based on the initial amount of chitin, which is lower than that reported by Pereira, Muniz,& Hsieh [30]. TEM images revealed acicular objects with a length ranging between 200 and 800 nm and a width between 20 and 80 nm (**Figure 1A**). Each particle appears to be constituted of a few parallel elementary rodlike crystallites that were not separated during the preparation treatment, as was also reported for cellulose nanocrystals of various origins [31]. The DLS profile showed a monomodal distribution with a hydrodynamic diameter extending from 50 to 200 nm and centered around 100 nm (**Figure 1B**). The surface charge of ChNCs depended on the pH (**Figure 1C**). ChNCs were positively charged with a ζ-potential exceeding 20 mV for pH lower than 6, and within pH range of 7.5 to 9, they were nearly neutral as their ζ-potential was lower

than ±5 mV. The pH dependence of the surface charge is due to the presence of amino groups on the surface of ChNCs that protonate at $pH < pK_{NH2}-1$ (with $pK_{NH2} \approx 6$). These surface charges strongly affected the colloidal stability and the optical transparency of ChNC suspensions. Within the pH range 3-6, the ζ-potential over +20 mV was enough to ensure high colloidal stability by electrostatic effect and high transparency of the ChNC suspension. Over pH 6.5, the surface charges were not strong enough to prevent the aggregation of ChNCs and the suspension turned hazy to turbid (**Figure 3S**).

The wettability of ChNCs was assessed by dynamic water contact angle measurement on the surface of ChNC films prepared by casting and drying. The contact angle was around 55° and remained unchanged over 1 min (**Figure 1D**). This value is in agreement with that around 50° reported by Gandini et al. [32]. Although this value denotes a hydrophilic surface, it is sufficient to ensure the partial wetting of oil droplet in emulsion. This higher value in comparison with cellulose-based films (around 20-30°) [33], can be essentially explained by the presence of N-acetyl groups on the surface of ChNCs. The contact angle and the surface hydrophilicity of chitin-based surface is controlled by the proportion of hydrophobic N-acetyl groups to that of hydrophilic amino groups, which is assessed through the degree of deacetylation (DD). In the present work, the DD of the ChNCs was 9.3 % (**Figure 2S**), meaning that about 90 % of the N-acetyl groups were not hydrolyzed. This explains the contact angle value of the ChNC film at around 55°.

**Figure 1C** indicates that the surface tension (γ) for a ChNC content up to 2 wt% did not notably decrease with a surface tension lower than 63 $mN\,m^{-1}$, meaning that no ChNC was adsorbed at the air-water interface resulting in no surface activity. This result disagrees with that reported by Tzoumaki et al. [17] who pointed out a decrease in γ in the presence of ChNCs, reaching about 44 $mN\,m^{-1}$ for a 1 wt% aqueous ChNC suspension. Two reasons might justify this discrepancy. The first one is that the ChNC suspension was left during 24h in contact with the platinum ring before the measurements were made. In our case, the measurement was rapidly performed. The second one is the difference in ionic strength which is known to strongly affect the interfacial behavior of polysaccharide-based NPs. It has recently been demonstrated that the air/water interfacial adsorption for nanocelluloses was diffusion-limited and salt-triggered [34].

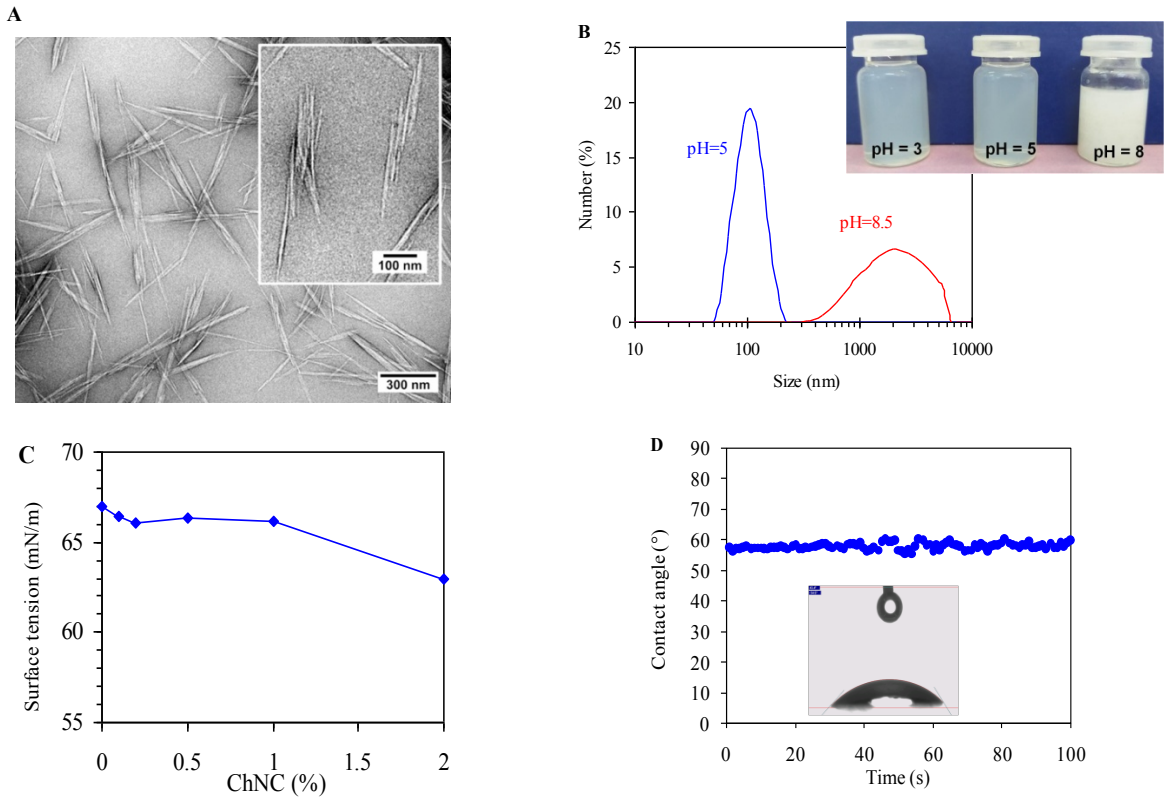


**Figure 1.** (A) TEM image of a negatively stained preparation of ChNCs at pH 6; (B) particle size distribution at pH 5 and pH 8.5; (C) surface tension *vs* ChNC content, and (D) contact angle of water *vs* time on a ChNC film.

### *3.2. Emulsification efficiency of ChNCs*

Emulsions at 15 wt% oil concentration and different ChNC contents were prepared using ASO, ESO and SO, adopting the same procedure in the presence of an increasing concentration of ChNCs. For the three oils, a stable emulsion was obtained at a ChNC concentration higher than 0.35 wt%. However, the size of the emulsion droplets notably evolved depending on the oil type and ChNC content (**Figure 2A-C**). For a given ChNC amount, the smaller droplets were observed for ESO followed by ASO and SO for which the size of the droplet remained quite large, exceeding 900 nm at 2 wt% ChNCs. Another key result is the decrease in the size of the emulsion oil droplets with increasing amount of ChNCs. For instance, at 0.35 wt% ChNCs, the average size reached 712 and 531 nm for ASO and ESO, respectively, and decreased to about 490 and 180 nm as the amount of ChNCs increased to 1.5 wt%. This dependence of the droplet size on the ChNC concentration evidenced their efficiency as a Pickering stabilizer in O/W emulsions, which is in agreement with previous works [17,19].

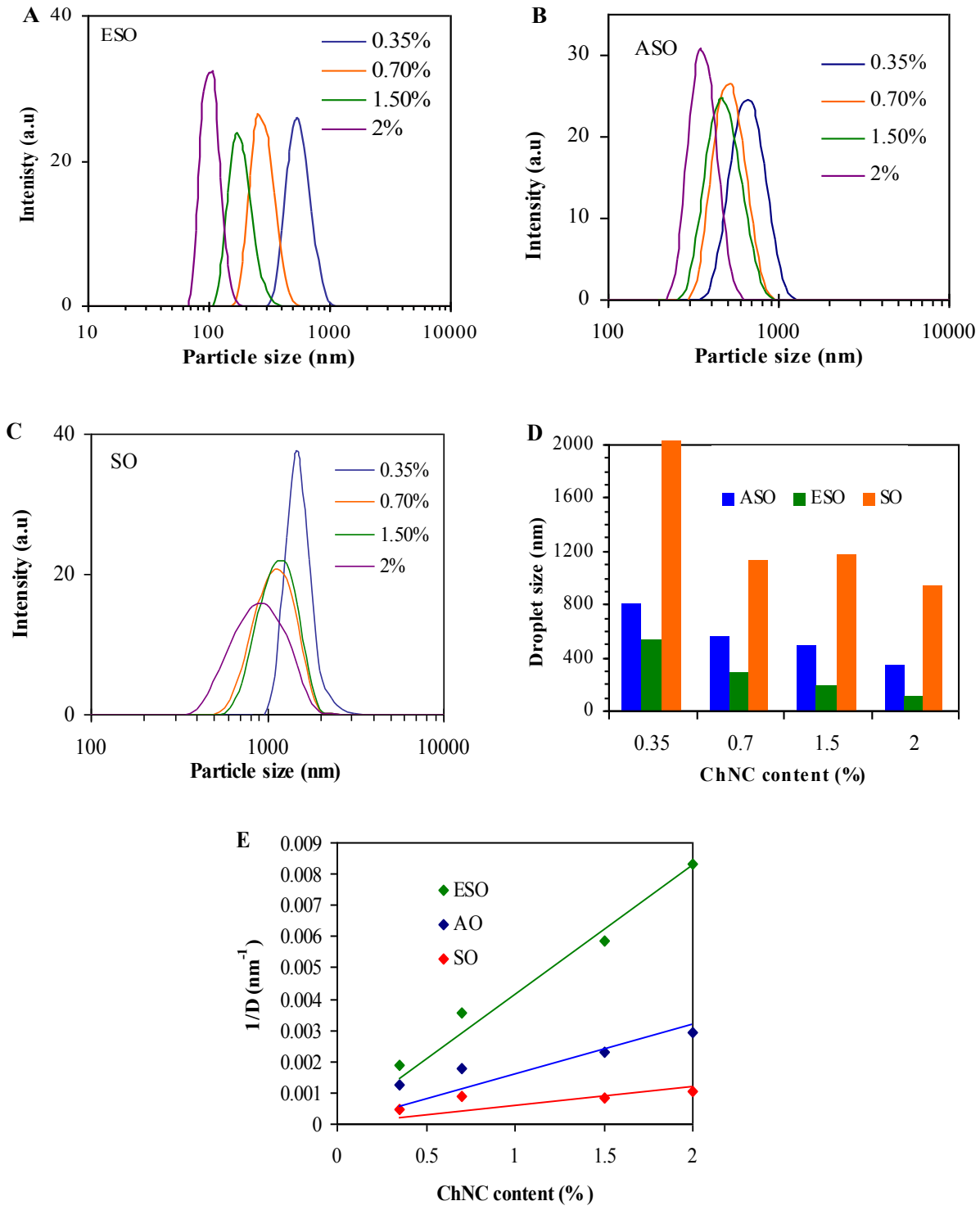


**Figure 2.** (A,B,C) Droplet size distribution for ESO, ASO and SO, emulsion at different ChNC content (wt%). (D) Mean droplet size of ASO, ESO and SO emulsion as a function of amount of added ChNCs, and (E) evolution of 1/D *vs* ChNC content for the corresponding emulsion. Oil concentration: 15 wt%.

With increasing ChNC concentration, more particles adsorbed at the oil-water interface and smaller droplets were generated. This dependence is often expressed by the proportionality between the inverse of the diameter of the oil droplet and the concentration in solid particles. Presently, this correlation shows a satisfactory fit of the inverse diameter of the oil droplet *vs* ChNC content over the whole investigated domain (**Figure 2E**). The slope of 1/D *vs* ChNC content differed according to the type of oil, with the highest slope observed for ESO followed by ASO and SO for which a nearly flat curve was obtained. This indicates a strong dependence of the droplet size with ChNC content for ESO and ASO, while the effect is much less pronounced for SO. One possible reason explaining this behavior is the difference in the interaction of ChNCs with the oil droplet, depending on the oil chemical structure. The stronger the interaction of ChNCs with the oil phase, the more efficient their stabilizing efficiency. Over a pH domain between 6 to 3, the surface of ChNCs is dominated by OH, $NHCH_3$ and $NH_3^+$groups. The presence of epoxy groups in ESO and hydroxyl groups in ASO promote the interaction with ChNCs through polar and hydrogen bonding, thus favoring the adsorption of ChNCs on the ESO and ASO droplets. On the other hand, this type of interaction did not exist with apolar SO, where a merely dispersive interaction between ChNCs and oil is likely to occur. However, due to its 3-membered O-ring structure, the interaction between the oxygen of the epoxy and the $NH_3^+$ and OH groups of ChNCs is more favored than with ASO and SO.

On the basis of the above discussion, we infer that the microstructure of the Pickering emulsion differs depending onto the type of oil. The most favorable interaction occurs between ESO and ChNCs thanks to the presence of epoxy groups that promote an interaction by polar and hydrogen bonding between the $NH^{3+}$and OH groups of ChNCs and ESO droplets, resulting in an effective coating of the oil droplets with ChNCs fibrils. In the presence of ASO, a fraction of ChNCs are attached to the oil droplet, mainly through hydrogen bonding between OH groups of ChNCs and those of ASO, leaving the unbound ChNCs in the continuous water phase. A connected network is held between the adsorbed and the ChNCs in the continuous phase, and the connectivity degree of the network increases as a higher amount of ChNCs is added. For the SO emulsion, the interaction between the oil droplets and the ChNCs is less favored, leaving a high fraction of ChNCs free in the water phase. The microstructure of the Pickering emulsion for the three oils is depicted in **Scheme 1**.

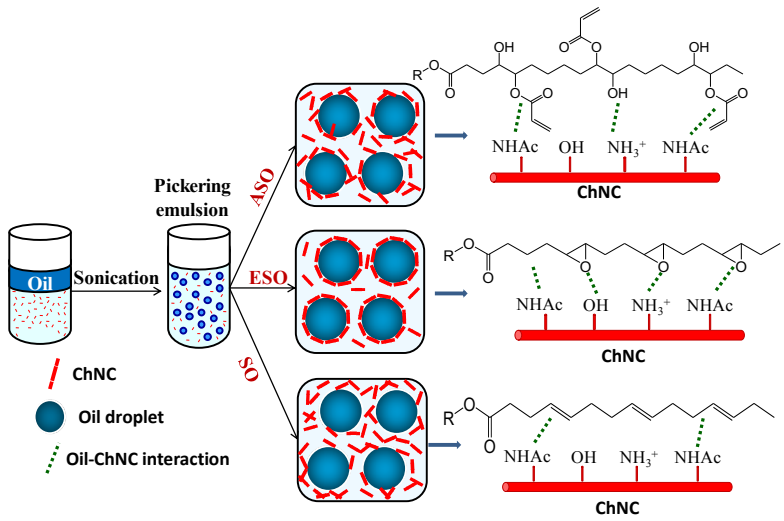


**Scheme 1.** Illustration of the stabilization modes of (A) ASO, (B) ESO, and (C) SO by ChNCs.

*3.3.Rheological behavior*

The rheological properties of the emulsions were investigated in the linear and non-linear domain by oscillatory sweep measurements of the storage modulus (G′) and loss modulus (G″) as a function of strain amplitude (γ) or frequency (f), and ii) in large strains by measuring the steady-state viscosity *vs.* shear rate.

The steady-state viscosity as a function of the shear rate for ASO, ESO, SO emulsion, and ChNC suspension is shown in **Figure 3**. For all emulsions, the viscosity decreased with increasing shear rate which is typical of a shear-thinning behavior. This property, frequently observed in Pickering emulsions, is explained by the formation of a weak droplet-solid particles network holding the dispersed phase [35]. As the shear rate increases, the hydrodynamic forces increase, causing the droplets to align with the shear field, thus reducing the possibility of interaction and resulting in a decrease in viscosity. At low shear rates, the viscosity increases as $\eta \approx \dot{\gamma}^{-1}$ as a function of the shear rate ($\dot{\gamma}$). Then, the shear stresses ($\tau$) tends to a constant value because $\tau = \eta\dot{\gamma} = \dot{\gamma}^{-1}\dot{\gamma} = constant = s$ for low shear rates, which corresponds to the yield stress. The materials behave like a gel resulting from the generation a connected network that prevents the flow. The presence of a yield stress is consistent with the observations of an elastic modulus higher than the viscous modulus, as will be confirmed by measurements in oscillatory regime. This yield stress which measures the cohesion of the connected network increases with the ChNC content. The ASO emulsion has a significantly higher cohesive stress than ESO and AO emulsions. At 2 wt% ChNCs, the yield stresses are *s*=13Pa for ASO, *s*=4 Pa for ESO, and *s*=0.35 Pa for SO. The ChNC suspension also exhibits a shear-thinning behavior over the whole

solid content from 0.35 to 2 wt%, in line with the literature data [36,37]. The ChNC suspensions did not seem to show the presence of a yield stress, and the viscosity decreases with a slope of approximately -0.7 over the entire shear rate range. This suggests the absence of a connected network among ChNCs.

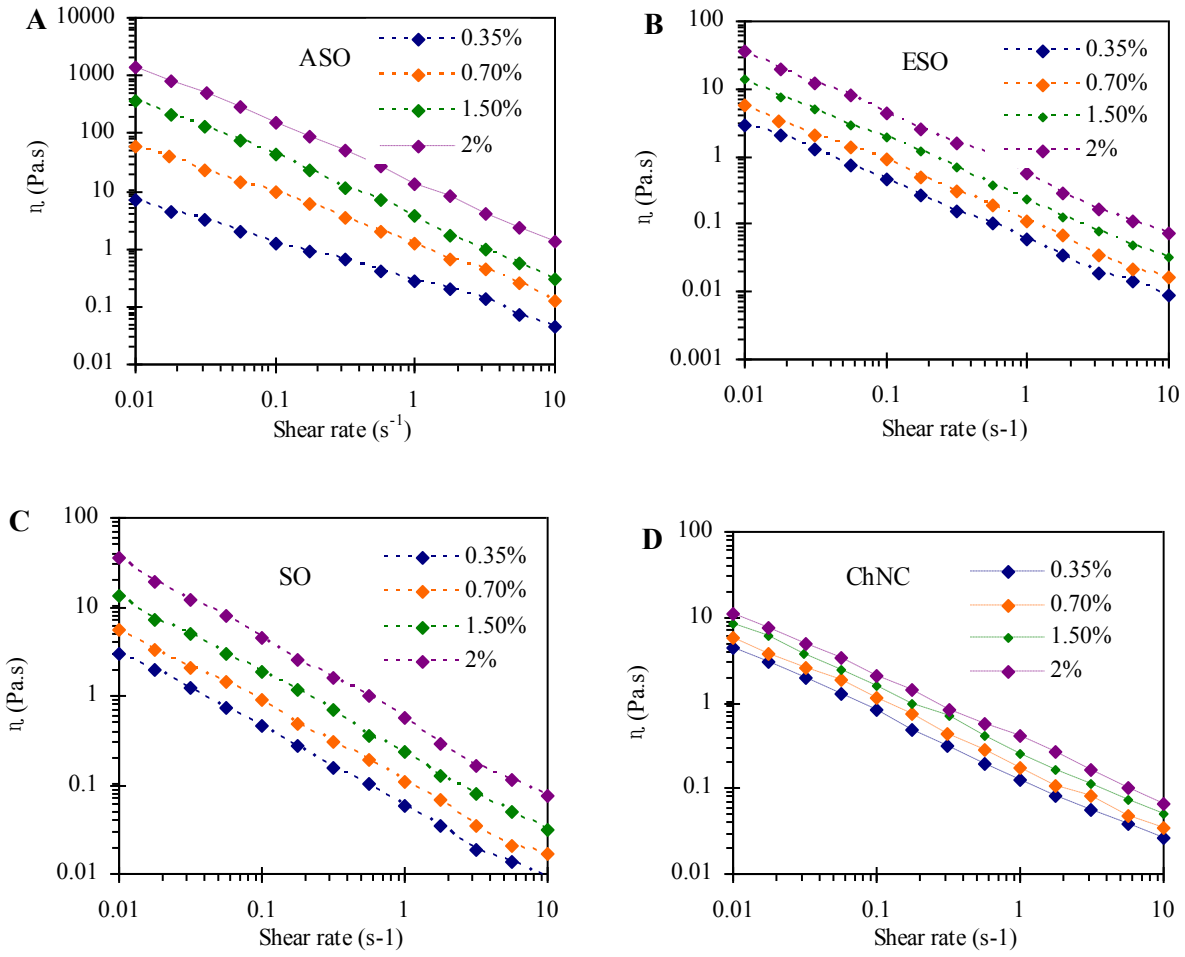


**Figure 3.** Viscosity as a function of shear rate for emulsions made of (A) ASO, (B) ESO, (C) SO, with different ChNC contents. (D) Viscosity of ChNC suspensions at different concentrations.

For all emulsions, the viscosity was shifted to a higher value as the concentration of added ChNCs increased, with a much more marked effect for ASO. This evolution was better highlighted by plotting the viscosity at 0.1 $s^{-1}$ for the different emulsions (**Figure 4S**). Two phenomena might explain this evolution. The first one is the decrease in the droplet size as the ChNC concentration increases, resulting in favorable droplet-droplet interaction and increasing frictional losses during flowing. The second effect might result from the increasing concentration of free ChNCs in the continuous phase as more ChNCs are added to the emulsion. Since not all

ChNCs are adsorbed on the oil droplets, a fraction of the particles remains in the aqueous phase, contributing to the increase in the viscosity of the continuous phase. However, this later effect would presumably not contribute to a large extent to the viscosity of the emulsion, considering that the viscosity of the ChNC suspension increased only 3.3 times when the concentrations in ChNCs increased from 0.35 to 2% at a shear rate 1 $s^{-1}$ (**Figure 3D**).

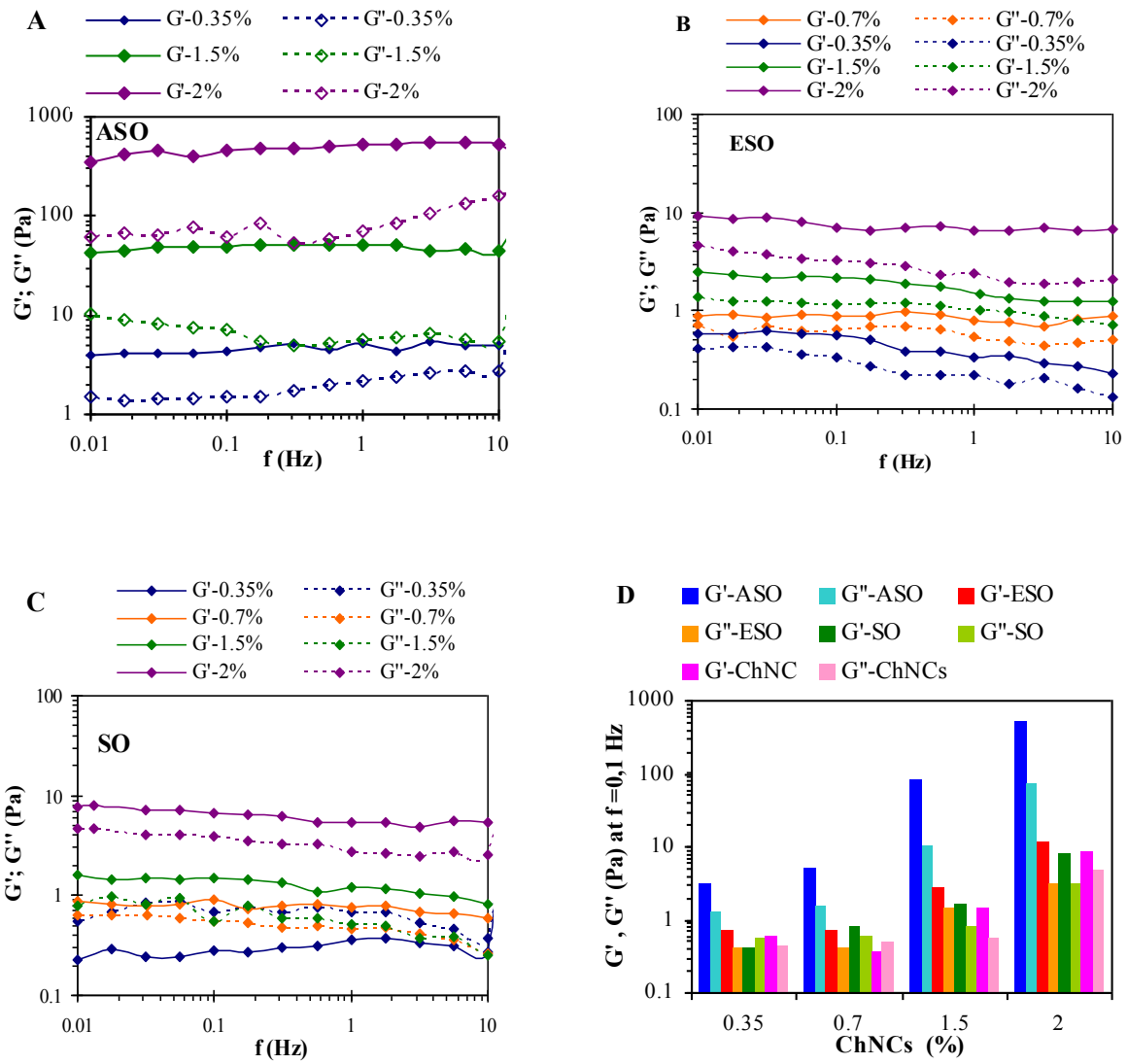


**Figure 4.**(A,B,C) Frequency sweeps for ASO, ESO and SO emulsions at different concentrations of ChNCs, and (D) G′ and G″ at 0.1 Hz for the different emulsions and ChNC suspensions.

Given the gel-like aspect of the emulsions, which was confirmed by the measurement of the yield stress at low shear rate of emulsions as established previously, the rheological properties

under dynamic conditions were worth investigating by an oscillatory sweep measuring of the storage modulus (G′) and loss modulus (G″) as a function of frequency (f) in the linear regime and strain amplitude (γ) (**Figures 4** and **5**). In the domain of linear elasticity, (i.e. in the range of strain where G' and G" are independent of the strain) (Figure 5), ASO and ESO emulsions, G′ and G″ were nearly frequency-independent, with G′ being higher than G″, confirming a gel-like behavior of the emulsion as had been established by the study of the evolution of viscosity at low the shear rates and the existence of yield stress (**Figure 4A,B**). This property was less obvious for the SO emulsion and the gel-like aspect was observed mainly for composition with ChNC content above 0.7 wt% (**Figure 4C**). The gel-like property of the emulsion is indicative of the generation of three-dimensional networks that might result from different mode of interconnection including; droplet-droplet, ChNC-ChNC and ChNC-droplet. In Pickering emulsions, the gel aspect of the emulsion has been widely reported in the literature with different possible origins being proposed, such as droplet-bridging, particle network, and partial aggregation[38,39]. Referring to **Figure 4A,B,D**, the magnitude of G′ increased with the ChNC content, meaning that the network cohesion increased with the concentration of added ChNCs. However, the elastic character of the ASO emulsion is much more marked than that of ESO or SO emulsions, suggesting a strong elastic character.

To further investigate the microstructure of the Pickering emulsion and reveal the transition from the linear to non-linear viscoelastic domain, the strain amplitude sweep was also measured. The plot of G′ vs strain was normalized with respect to the linear viscoelastic region (LVR), to better highlight the transition domain (**Figure 5**). For all emulsions, G′ showed a plateau up to a critical strain $\gamma_c$ above which G′ abruptly declined, marking the structural breakdown of the emulsion microstructure and the transition from a solid to a fluid material. For all emulsions, $\gamma_c$ increased with increasing ChNC content, indicating the development of a stronger gel network structure. Likewise, $\gamma_c$ value differs according to the type of oil, with the highest degree reached with ASO, followed by ESO and SO (**Figure 5A-C**). For instance, at 12 wt% ChNCs, $\gamma_c$ was around 2 %, 0.8 % and 0.2 % for ASO, ESO and SO emulsions, respectively. It is worth noting that for ChNCs suspension, nearly no LVR was noted below a concentration of 2 wt% and a weak LVR with $\gamma_c$ around 0.1 % was observed for a suspension at 2 wt% ChNCs (**Figure 5D**), meaning that ChNCs are less inclined to set-up interconnected networks within the studied concentration range and that interconnected networks form in the emulsion once oil droplets are in contact with ChNCs.

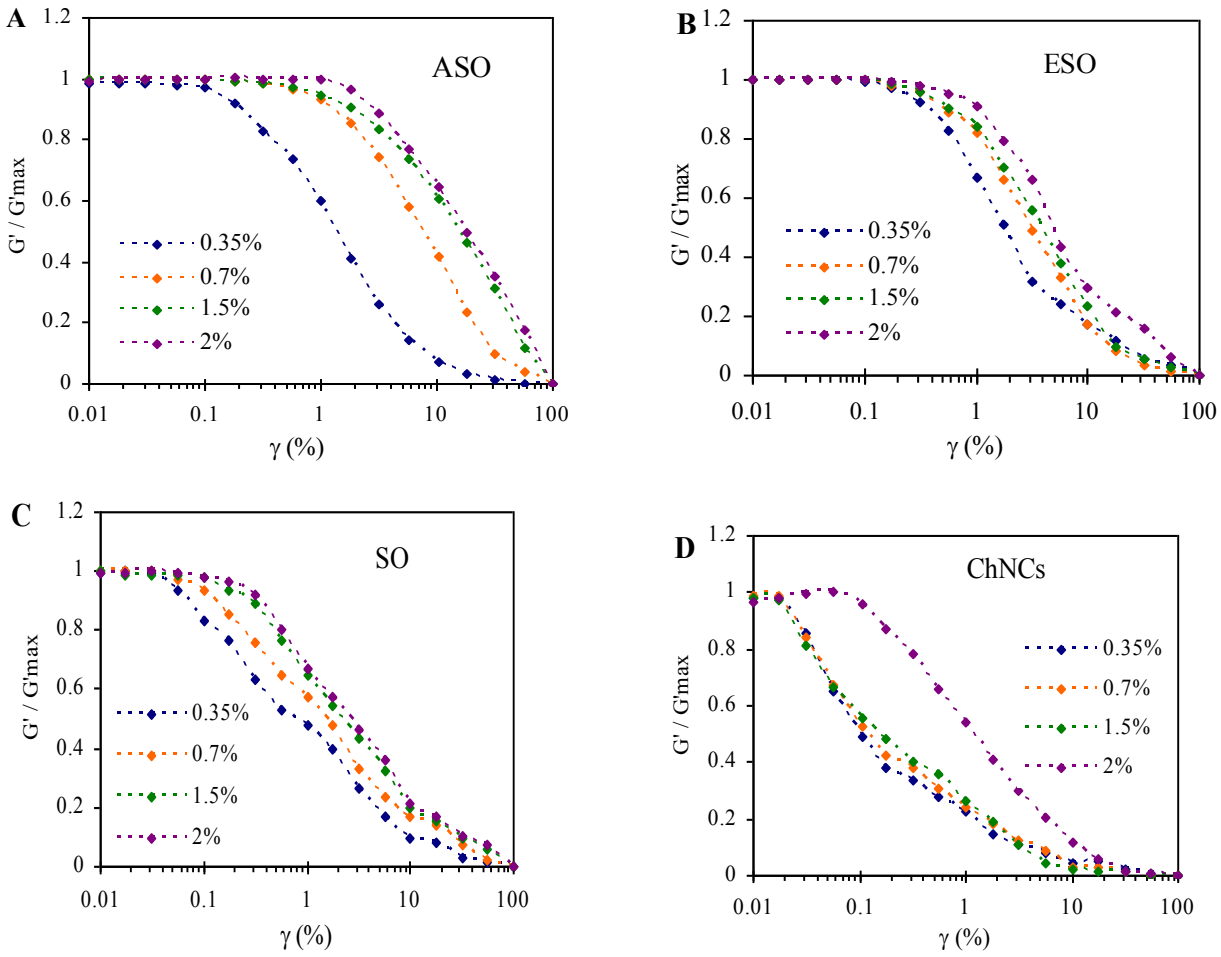


**Figure 5.** Strain amplitude sweep results at f = 0.1 Hz for Pickering emulsions of (A) ASO, (B) ESO, (C) SO, at different ChNC contents, and (D) for ChNC suspensions at different concentrations.

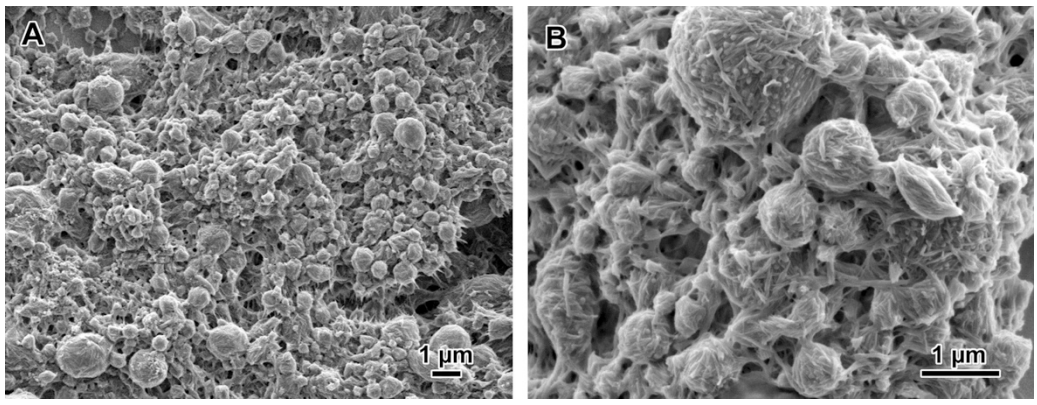


**Figure 6.**A,B) SEM images of an ASO emulsion stabilized with 1.5 wt% ChNCs. The emulsion containing 1% Irgacure 184 photoiniator was exposed to UV-light for 1 min to induce crosslinking in oil droplets.

The surface coating of the oil droplets by ChNCs and the formation of a network connecting ChNCs were assessed by SEM observation for the ASO emulsion rigidified by UV irradiation. Such treatment was not possible for ESO and SO given their liquid form and the impossibility to harden the droplet by UV or other external action. The images in **Figure 6** show polydisperse droplets of crosslinked ASO were fully covered by ChNCs lying flat on the droplet surface. Outside of the droplets, a fraction of the ChNCs formed a percolating network partially embedding the particles. Since the excess of free ChNCs has been removed by washing, this network was likely formed in the emulsion and not upon drying. These images support the hypothesis concerning the organization of ChNCs around oil droplets for ASO as depicted in **Scheme 1**.

*3.4. Storage stability*

The stability of the emulsion over time was studied by monitoring the particle size of the emulsion over one month storage at 25 °C and the visual evolution of the emulsion aspect over time (**Figures 7** and **5S**). Different behaviors were observed according to the oil nature and ChNC content: for ASO and ESO, the emulsions looked stable without evolution of their aspect and without any sign of creaming when the ChNC content exceeded 1.5 wt%. Below this level, a creaming of the emulsion was observed, without any visible sign of oil-floating (oil-layering) during a 1-month storage. Over one month, the particle size analysis revealed no significant evolution, in oil droplet size for ASO and ESO emulsions as the content in ChNCs exceeded 1.5 wt% (**Figure 5S**). These data further supported the effectiveness of ChNCs in stabilizing O/W emulsions based on ESO and ASO, as long as their content exceeded a critical level. The tendency was different for SO, where a creaming was noticed after one week standing for all emulsions, irrespective of the ChNC content, with oil-layering observed for emulsions with a ChNC content lower than 0.7 wt%. The size of oil droplet increased also with time; especially with a ChNC content lower than 0.7 wt% and after one month storage. The gel-like character of ASO and ESO emulsions when the content in ChNCs was higher than1.5 wt% is another parameter accounting for the better resistance to creaming of these emulsions, by providing a physical barrier to restrain the movement of oil droplets.

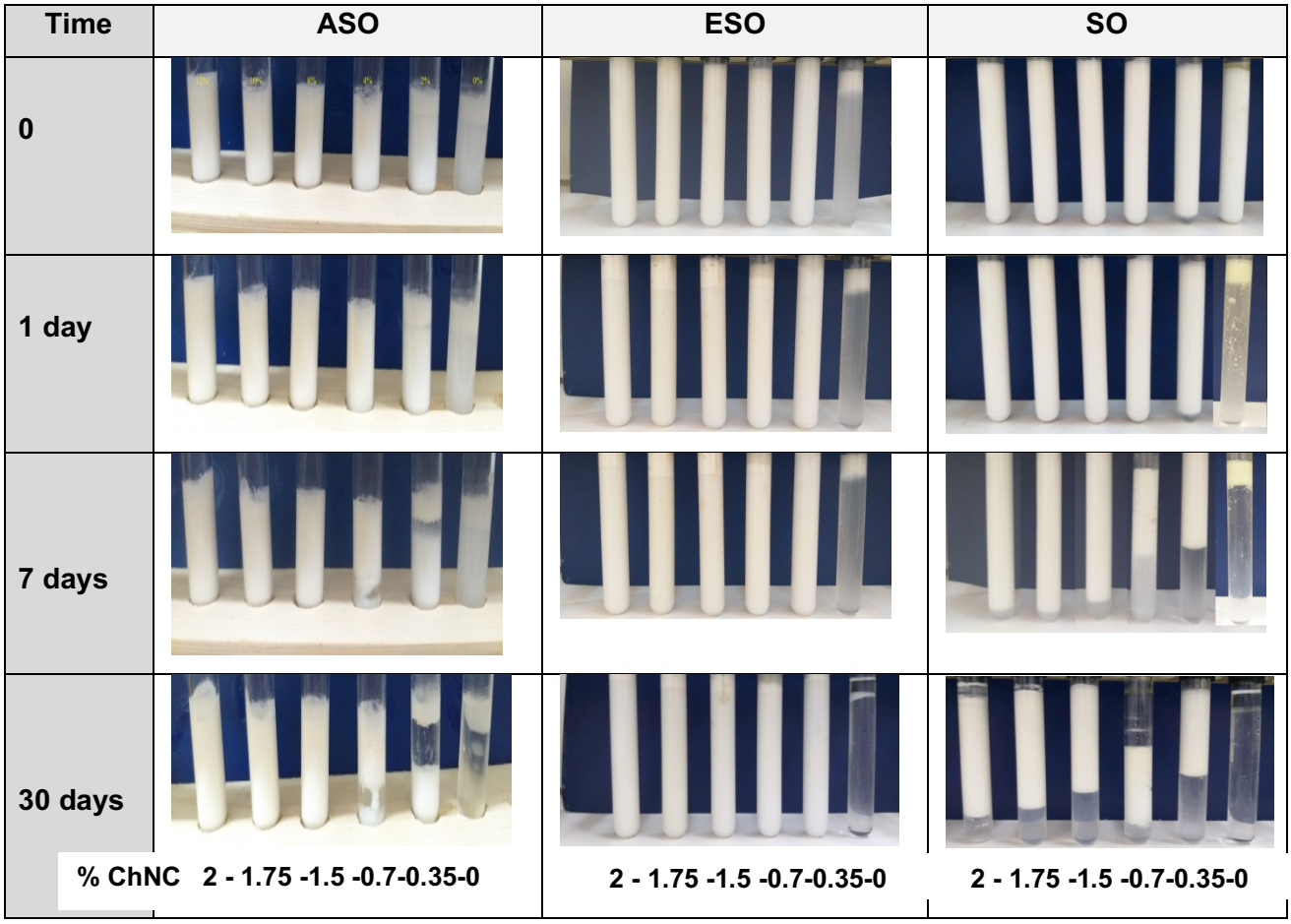


**Figure 7.**Change in the aspect of the emulsion with storage time, according to the oil type and ChNC content (from left to right): 2, 1.75, 1.5, 0.7, 0.35 and 0 wt% ChNCs based on the water phase). Oil fraction: 0.15.

*3.5. Effect of the oil content*

The effect of the oil phase fraction on the emulsion property has been studied with ASO by preparing emulsions at an oil fraction from 15 to 30 wt% and using the same amount of ChNCs with respect to the oil phase. The mean droplet size did not markedly change with the increase in oil fraction within the range between 15 and 30 wt%, reaching about 460, 400 and 520 nm for emulsion with an oil phase fraction of 15, 20 and 30 wt%, respectively (**Figure 6S**). This effect is expected for two reasons, (i) the increases in the interfacial oil/water area requiring additional ChNCs to stabilize oil droplets, and (ii), the increment in the oil fraction increases the probability of droplets collision as dispersed particle became closer. Since the amount of ChNCs was kept constant (1.5 wt%), while increasing the oil fraction, it is coherent to observe the trend reported in **Figure 6S**. This indicates that the ChNC/oil phase ratio seems to play a key role in determining the emulsion droplet size, which is typical of emulsions stabilized by solid particles [19]. The gel-like aspect of the emulsion increased with the oil phase fraction, indicating the

formation of a stronger network structure. The strengthening in the elastic character was notable when the oil fraction grew from is doubled from 15 to 30 %, with more than 10-fold increase in G' (**Figure 6S**). The strengthening of the emulsion network is likely due to the increase in the number of oil droplet in the continuous phase reducing the interdistance between neighboring droplets which results in setting up a denser network.

The possibility to use ChNCs as Pickering stabilizer in O/W emulsions based on reactive oils such as ASO and ESO opens new possibilities to produce waterborne nanocomposite dispersion for UV-curing (for ASO) and 2K (for ESO) coating application. Beyond their emulsification efficiency, the inclusion of ChNCs [40] is expected to impart beneficial effect on the coated film by enhancing the stiffness, scratch resistance and barrier properties. Work is under progress to investigate the effect of ChNC inclusion on the properties of UV-curable acrylated soybean oil coatings. Moreover, considering the numerous benefits of ChNCs that include their natural origin, environment-friendly character, antibacterial activity, safety, biodegradability and easy production, we believe that the use of ChNCs as emulsion stabilizer in substitution of synthetic surfactants will open new horizons to develop a wider range of emulsions for cosmetics, adhesives, coating and food.

It is worth noting that compared to the previously published data about the aptitude of ChNCs to stabilize O/W emulsions via a Pickering effect, the present work shed light on the key role of oil droplet/ChNCs interaction in controlling the droplet size, rheology and long term stability of the emulsion. In fact, in most of the reported literature data, apolar oils (dodecane, hexadecane) or triglycerides without any polar groups, such as sunflower or corn oil, were mainly used, and the published data were basically limited to demonstrate the possibility to use ChNCs as a solid stabilizer, without emphasis on key role of ChNC-droplet interaction on the properties of the resulting emulsion. In the present article, we have shown that oils bearing polar groups strongly enhanced the emulsification efficiency of ChNCs with a possibility to form emulsions with nanoscale droplets over a critical amount of ChNC content.

## 4. Conclusion

The emulsification of soybean oil (SO), epoxidized soybean oil (ESO) and acrylated epoxidized soybean oil (ASO)in water using ChNCs as sole stabilizing agent was investigated. Above 0.7 wt% ChNC content, a stable O/W emulsion was obtained by short sonication of the oil-water mixture. The properties of the emulsions differed depending on the oil chemical structure. The smaller oil droplets were formed with ESO followed by ASO and SO that

produced emulsions with micrometer-size droplets. Rheology analyses under dynamic conditions indicated a dominant gel-like character for ESO and ASO emulsions with increment in the elasticity with increasing ChNC content, while this effect was less marked for SO. This difference is indicative of the generation of interconnected network structures in the presence of ASO and ESO as the oil phase. Above 1.5 wt% ChNC content, emulsions stable over one month, without any sign of creaming, were obtained with ESO and ASO, while a creaming without oil-off effect was noted in presence of SO. The difference in the emulsion properties according to the oil chemical structure was explained by the difference in the mode of interaction between ChNCs and the oil droplets. In ASO and ESO, the presence of hydroxyl and epoxy groups promoted the interaction through polar effect between $NH^{3+}$ and OH groups in ChNCs and the oil droplets, favoring their adsorption on the oil droplet with the generation of a network which further improved the long-term stability by entrapping the oil droplet within the network and preventing their coalescence.

**Acknowledgements**

We thank Pr. Emmanuel Belamie (ICGM, Montpellier, France) for providing the detailed method of ChNC preparation. The authors acknowledge LabEx Tec 21(Investissements d'Avenir #ANR-11-LABX-0030), as well as the PHC Utique 19G1123 and Glyco@Alps programs (Investissementsd'Avenir#ANR-15-IDEX-02) for financial support. We thank the NanoBio-ICMG Platform (FR 2607, Grenoble) for the use of the Electron Microscopy facility, and Christine Lancelon-Pin (CERMAV) for the SEM observations. CERMAV and LRP are part of Institut Carnot PolyNat (Investissements d'Avenir #ANR-11-CARN-030-01).

**Appendix A. Supplementary Data.**

Supplementary material related to this article can be found, in the online version, at https://doi.org/10.1016/j.colsurfb.2021.111604

## References

[1] B. Kronberg, K. Holmberg, B. Lindman, Emulsions and emulsifiers. Surface Chemistry of Surfactants and Polymers, John Wiley & Sons, Ltd., West Sussex, UK, 2014.

[2] D. Georgieva, V. Schmitt, F. Leal-Calderon, D. Langevin, On the possible role of surface elasticity in emulsion stability, Langmuir 25 (2009) 5565–5573.

[3] E. Dickinson, Hydrocolloids as emulsifiers and emulsion stabilizers, Food Hydrocoll. 23 (2009) 1473–1482.

[4] I. Capron, B. Cathala, Surfactant-free high internal phase emulsions stabilized by cellulose nanocrystals, Biomacromolecules 14 (2013) 291–296.

[5] I. Kalashnikova, H. Bizot, B. Cathala, I. Capron, New Pickering emulsions stabilized by bacterial cellulose nanocrystals (BCN), Langmuir 27 (2011) 7471–7479.

[6] N. Nikfarjam, N.T. Qazvini, Y. Deng, Surfactant free Pickering emulsion polymerization of styrene in w/o/w system using cellulose nanofibrils, Eur. Polym. J. 64 (2015) 179–188.

[7] K. Xhanari, K. Syverud, P. Stenius, Emulsions stabilized by microfibrillated cellulose: the effect of hydrophobization, concentration and o/w ratio, J. Dispers. Sci. Technol. 32 (2011) 447–452.

[8] C. Li, Y. Li, P. Sun, C. Yang, Starch nanocrystals as particle stabilisers of oil-in-water emulsions, J. Sci. Food Agric. 94 (2014) 1802–1807.

[9] B.B. Sanchez de la Concha, E. Agama-Acevedo, A. Aguirre-Cruz, L.A. Bello-Pérez, J. Alvarez-Ramírez, OSA esterification of amaranth and maize starch nanocrystals and their use in "Pickering" emulsions, Starch/Staerke 72 (2020), 1900271.

[10] S. BelHaaj, W. Thielemans, S. Boufi, Starch nanocrystals and starch nanoparticles from waxy maize as nano-reinforcement: a comparative study, Carbohydr. Polym. 143 (2016) 310–317.

[11] S. BelHaaj, W. Thielemans, A. Magnin, S. Boufi, Starch nanocrystal stabilized Pickering emulsion polymerization for nanocomposites with improved performance, ACS Appl. Mater. Interfaces 6 (2014) 8263–8273.

[12] S. BelHaaj, W. Thielemans, S. Boufi, Starch nanoparticles produced via ultrasonication as a sustainable stabilizer in Pickering emulsion polymerization, RSC Adv. 4 (2014) 42638–42646.

[13] S. BelHaaj, A. Ben Mabrouk, W. Thielemans, S. Boufi, A one-step miniemulsion polymerization route towards the synthesis of nanocrystal-reinforced acrylic nanocomposites, Soft Matter 9 (2013) 1975–1984.

[14] R.J.G. Lopetinsky, J.H. Masliyah, Z. Xu, Solids-stabilized emulsions: a review, in: B. P. Binks, T.S. Horozov (Eds.), Colloidal Particles at Liquid Interfaces, Cambridge University Press, 2006. Chap. 6.

[15] T. Tadros, Encyclopedia of Colloid and Interface Science, Springer-Verlag, Berlin Heidelberg, 2013.

[16] A.M. Salaberria, J. Labidi, S. Fernandes, Different routes to turn chitin into stunning nano-objects, Eur. Polym. J. 68 (2015) 503–515.

[17] N. Butchosa, C. Brown, P.T. Larsson, L.A. Berglund, V. Bulone, Q. Zhou, Nanocomposites of bacterial cellulose nanofibers and chitin nanocrystals: fabrication, characterization and bactericidal activity, Green Chem. 15 (2013) 3404–3413.

[18] M.V. Tzoumaki, T. Moschakis, V. Kiosseoglou, C. Biliaderis, Oil-in-water emulsions stabilized by chitin nanocrystal particles, Food Hydrocoll. 25 (2011) 1521–1529.

[19] C. Jiménez-Saelices, T. Trongsatitkul, D. Lourdin, I. Capron, Chitin Pickering emulsion for oil inclusion in composite films, Carbohydr. Polym. 242 (2020), 116366.

[20] X. Wang, K. Liang, Y. Tian, Y. Ji, A facile and green emulsion casting method to prepare chitin nanocrystal reinforced citrate-based bioelastomer, Carbohydr. Polym. 157 (2017) 620–628.

[21] M.R. Barkhordari, M. Fathi, Production and characterization of chitin nanocrystals from prawn shell and their application for stabilization of Pickering emulsions, Food Hydrocoll. 82 (2018) 338–345.

[22] K. Pang, B. Ding, X. Liu, H. Wu, Y. Duan, J. Zhang, High yield preparation of a zwitterionically charged chitin nanofiber and its application in a doubly pH-responsive Pickering emulsion, Green Chem. 19 (2017) 3665–3670.

[23] Y. Huang, J. Yang, L. Chen, L. Zhang, Chitin nanofibrils to stabilize long-life Pickering foams and their application for lightweight porous materials, ACS Sustain. Chem. Eng. 6 (2018) 10552–10561.

[24] Y. Zhu, S. Huan, L. Bai, A. Ketola, X. Shi, X. Zhang, J.A. Ketoja, O.J. Rojas, High internal phase oil-in-water Pickering emulsions stabilized by chitin nanofibrils: 3D structuring and solid foam, ACS Appl. Mater. Interfaces 12 (2020) 11240–11251.

[25] E. Perrin, H. Bizot, B. Cathala, I. Capron, Chitin nanocrystals for Pickering high internal phase emulsions, Biomacromolecules 15 (2014) 3766–3771.

[26] L. Bai, S. Huan, W. Xiang, L. Liu, Y. Yang, R. Wahyu, Y. Fan, O.J. Rojas, Self-assembled networks of short and long chitin nanoparticles for oil/water interfacial superstabilization, ACS Sustain. Chem. Eng. 7 (2019) 6497–6565.

[27] N.K. Gopalan, A. Dufresne, Crab shell chitin whisker reinforced natural rubber nanocomposites. 1. Processing and swelling behavior, Biomacromolecules 4 (2003) 657–665.

[28] L. Raymond, F.G. Morin, R.H. Marchessault, Degree of deacetylation of chitosan using conductometric titration and solid-state NMR, Carbohydr. Res. 246 (1993) 331–336.

[29] A. Magnin, J.M. Piau, Cone-and-plate rheometry of yield stress fluids. Study of an aqueous gel, J. Non-Newton. Fluid Mech. 36 (1990) 85–108.

[30] A.G. Pereira, E.C. Muniz, Y.L. Hsieh, Chitosan-sheath and chitin-core nanowhiskers, Carbohydr. Polym. 107 (2014) 158–166.

[31] S. Elazzouzi-Hafraoui, N. Nishiyama, J.-L. Putaux, L. Heux, F. Dubreuil, C. Rochas, The shape and size distribution of crystalline nanoparticles prepared by acid hydrolysis of native cellulose, Biomacromolecules 9 (2008) 57–65.

[32] A.G. Cunha, S. Fernandes, C.S.R. Freire, A.J.D. Silvestre, C.P. Neto, A. Gandini, What is the real value of chitosan's surface energy? Biomacromolecules 9 (2008) 610–614.

[33] M. Abdelmouleh, S. Boufi, M.N. Belgacem, A.P. Duarte, A.H. Ben Salah, A. Gandini, Modification of cellulosic fibres with functionalized silanes: development of surface properties, Int. J. Adhes. Adhes. 24 (2004) 43–54.

[34] P. Bertsch, M. Arcari, T. Geue, R. Mezzenga, G. Nyström, P. Fischer, Designing cellulose nanofibrils for stabilization of fluid interfaces, Biomacromolecules 20 (2019) 4574–4580.

[35] M. Anvari, H.S. Joyner, Effect of formulation on structure-function relationships of concentrated emulsions: rheological, tribological, and microstructural characterization, Food Hydrocoll. 72 (2017) 11–26.

[36] J. Li, J.F. Revol, R.H. Marchessault, Rheological properties of aqueous suspensions of chitin crystallites, J. Colloid Interface Sci. 183 (1996) 365–373.

[37] J. Li, J.F. Revol, E. Naranjo, R.H. Marchessault, Effect of electrostatic interaction on phase separation behaviour of chitin crystallite suspensions, Int. J. Biol. Macromol. 18 (1996) 177–187.

[38] L. Alison, P.A. Rühs, E. Tervoort, A. Teleki, M. Zanini, L. Isa, R.A. Studart, Pickering and network stabilization of biocompatible emulsions using chitosan-modified silica nanoparticles, Langmuir 32 (2016) 13446–13457.

[39] M.N. Lee, H.K. Chan, A. Mohraz, Characteristics of Pickering emulsion gels formed by droplet bridging, Langmuir 28 (2012) 3085–3091.

[40] A. Kaboorani, N. Auclair, B. Riedl, V. Landry, Mechanical properties of UV-cured cellulose nanocrystal (CNC) nanocomposite coating for wood furniture, Prog. Org. Coat. 104 (2017) 91–96.